Self-Assembly of Cationic, Tetranuclear, Pt(II) and Pd(II) Macrocyclic Squares. X-ray Crystal Structure of $[Pt^{2+}(dppp)(4,4'\text{-bipyridyl})2^{-}OSO_2CF_3]_4$†

Peter J. Stang,* Danh H. Cao, Shinichi Saito, and Atta M. Arif

Contribution from the Department of Chemistry, The University of Utah, Salt Lake City, Utah 84112

Received March 9, 1995®

Abstract: The preparation, characterization, and some chemistry of a series of unique cationic, tetranuclear, Pt(II)- and Pd(II)-based macrocyclic squares are reported. A variety of bidentate ligands (bipyridine, diazapyrene, dicyanobenzene, and dicyanobiphenyl) are interacted with the square-planar *cis*-bis(phosphine) Pt and Pd bis(triflate) complexes in organic solvents at room temperature, resulting in molecular squares in high isolated yields via self-assembly. All molecular squares are robust air- and water-stable microcrystalline solids with decomposition points mostly above 200 °C. They are generally soluble in polar organic solvents but not in water or nonpolar solvents like pentane, toluene, and ether. The cyano-based macrocycles are highly fluxional in solution, whereas the bipy and related systems are more stable. Concentration-dependent chemical shifts are observed for the ortho and meta protons of 1,5-dihydroxynaphthalene, indicating host–guest interactions and inclusion phenomena. X-ray crystal structures are reported for the molecular square $[(dppp)Pt(bipy)]_4^{8+}8^{-}OSO_2CF_3$ (**15a**), as well as a dinuclear dicyanobenzene complex **25** and the $[(dppp)M(pyrazine)]^{2+}2^{-}OSO_2CF_3$ (M = Pt, Pd) complexes **20a,b**.

Introduction

Supramolecular chemistry, self-assembly, inclusion phenomena, molecular recognition, and noncovalent interactions are at the forefront of modern chemistry. These phenomena are commonly accessed by various macrocyclic and related assemblies. Diverse macrocycles and hosts such as crown ethers, cyclophanes, cyclodextrins, calixarenes, cryptands, spherands, cavitands, carcerands, clathrates, cryptophanes, molecular clefts, and like species are well known.[1–10] The great majority of these macrocycles are conformationally reasonably flexible organic molecules that preferentially interact with cationic guests.[1–10] Much less is known about inorganic or organometallic macrocycles.

Recently, novel, conformationally more rigid, tetranuclear, cationic[11] macrocyclics, with ~90° bond angles, have emerged[12–17] as the newest members of the above family of supramolecular assemblies. Currently, two different types of such macrocyclic squares are known: (1) those based on a main group element with covalently bound iodine at the corners, as in **1**, and (2) transition metal-based squares with chelating ligands, as in **2**. In this paper, we report full details for the

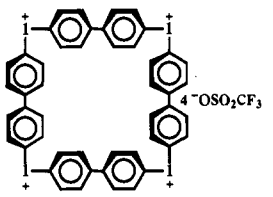

1

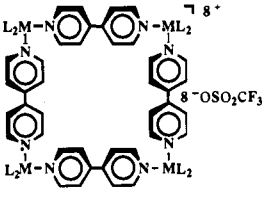

2

preparation, the spectral characterization, and the first X-ray crystal molecular structure for diverse transition metal-based, cationic, macrocyclic squares, **2**, along with some preliminary chemistry.

Results and Discussion

Preparation of Chelated, Square-Planar *cis*-Pt and *cis*-Pd Bis(triflate) Complexes, 2,7-Diazapyrene, and 2,9-Diazadibenzo[*cd,lm*]perylene. Chelation of $PtCl_2$ or $PdCl_2$ with either 1,3-bis(diphenylphosphino)propane (dppp) or triethylphosphine according to standard procedures[18,19] gave the respective *cis* complexes **4**, as outlined in Scheme 1. Reaction of **4** with excess $AgOSO_2CF_3$ in CH_2Cl_2 resulted in the desired bis(triflate) complexes **5**. These stable, albeit hygroscopic,

† Dedicated to Professor Manfred Regitz on the occasion of his 60th birthday.

® Abstract published in *Advance ACS Abstracts*, June 1, 1995.

(1) *Frontiers in Supramolecular Chemistry*; Schneider, H., Dürr, H., Eds.; VCH: Weinheim, 1991.

(2) *Monographs in Supramolecular Chemistry 1 and 2*; Stoddard, J. F., Ed.; Royal Society of Chemistry; Cambridge, 1989, 1991.

(3) *Supramolecular Chemistry*; Balzani, V., DeCola, L., Eds.; Kluwer Academic Publishers: The Netherlands, 1992.

(4) Vögtle, F. *Cyclophane Chemistry*; J. Wiley & Sons: Chichester, 1993.

(5) Diederich, F. *Cyclophanes*; Royal Society of Chemistry; Cambridge, 1991.

(6) *Calixarenes: A Versatile Class of Macrocyclic Compounds*; Vicens, J., Bohmer, V., Eds.; Kluwer Academic Publishers: The Netherlands, 1990.

(7) Gutsche, C. D. *Calixaranes*; Royal Society of Chemistry: London, 1989.

(8) *Inclusion Phenomena and Molecular Recognition*; Atwood, J. L., Ed.; Plenum: New York, 1990.

(9) *Molecular Inclusion and Molecular Recognition—Clathrates II*; Weber, E., Ed.; Topics in Current Chemistry 149; Springer-Verlag: New York, 1987.

(10) *Host–Guest Complex Chemistry: Synthesis, Structure, Applications*; Vögtle, F., Weber, E., Eds.; Springer-Verlag: Berlin, 1985.

(11) For an early, neutral, tetranuclear, organometallic macrocycle, see: Stricklen, P. M.; Vocko, E. J.; Verkade, J. G. *J. Am. Chem. Soc.* **1983**, *105*, 2494.

(12) Stang, P. J.; Zhdankin, V. V. *J. Am. Chem. Soc.* **1993**, *115*, 9808.

(13) Rauter, H.; Hillgeris, E. C.; Erxleben, A.; Lippert, B. *J. Am. Chem. Soc.* **1994**, *116*, 616.

(14) Stang, P. J.; Cao, D. H. *J. Am. Chem. Soc.* **1994**, *116*, 4981.

(15) Drain, C. M.; Lehn, J.-M. *J. Chem. Soc., Chem. Commun.* **1994**, 2313.

(16) Fujita, M.; Kwon, Y. J.; Washizu, S.; Ogura, K. *J. Am. Chem. Soc.* **1994**, *116*, 1151. Fujita, M.; Nagao, S.; Iida, M.; Ogata, K.; Ogura, K. *J. Am. Chem. Soc.* **1993**, *115*, 1574. Fujita, M.; Yazaki, J.; Ogura, K. *J. Am. Chem. Soc.* **1990**, *112*, 5645.

(17) Stang, P. J.; Whiteford, J. A. *Organometallics* **1994**, *13*, 3776.

(18) Appleton, T. G.; Bennett, M. A.; Tomkins, I. B. *J. Chem. Soc. D* **1976**, 439.

(19) Parshall, G. W. *Inorg. Synth.* **1970**, *12*, 27.

(20) Hunig, S.; Gross, J.; Lier, E. F.; Quast, H. *Liebigs Ann. Chem.* **1973**, 339–358.

0002-7863/95/1517-6273$09.00/0

Scheme 1. Formation of Square-Planar Chelated *cis*-Bis(triflate) Complexes

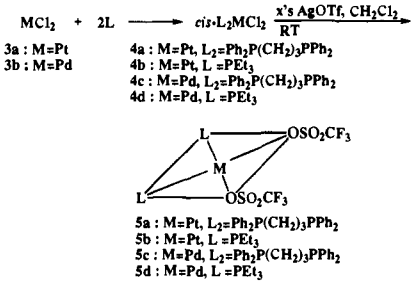

Scheme 2. Preparation of 2,7-Diazapyrene (**9**)

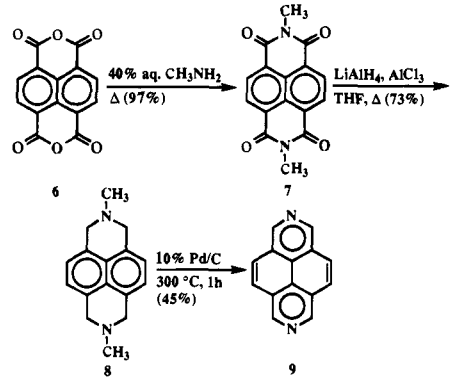

Scheme 3. Preparation of 2,9-Diazadibenzo[*cd*,*lm*]perylene (**13**)

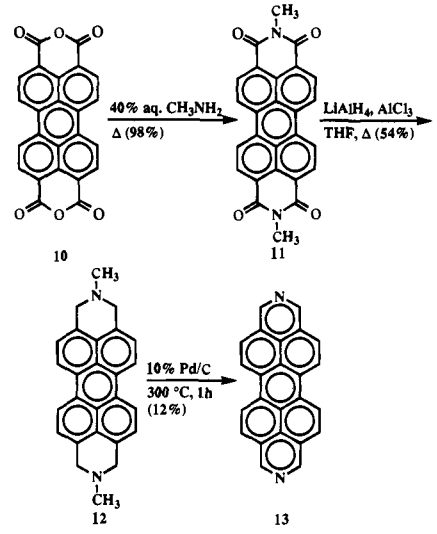

microcrystalline, bis(triflate) complexes were characterized by multinuclear NMR, IR, and physical means as described in the Experimental Section.

2,7-Diazapyrene (**9**) was prepared according to a modified literature[20] procedure, as outlined in Scheme 2. Commercially available 1,4,5,8-naphthalenetetracarboxylic dianhydride (**6**) was converted to the diimide **7**, which was reduced to **8** and aromatized with Pd/C to 2,7-diazapyrene (**9**). Likewise, 2,9-diazadibenzo[*cd*,*lm*]perylene (**13**) was prepared according to an analogous modified literature procedure[21] using commercially available 3,4,9,10-perylenetetracarboxylic dianhydride (**10**), as outlined in Scheme 3. Unfortunately, because of the low solubility of such polycyclic aromatics, including **13**, in all common solvents, the yield in the final aromatization step was only 12%.

(21) Slama-Schwok, A.; Jazwinski, J.; Bere, A.; Montenay-Garestier, T.; Rougee, M.; Helene, C.; Lehn, J.-M. *Biochemistry* **1989**, *28*, 3227−3234.
(22) Whitesides, G. M.; Simanek, E. E.; Mathias, J. P.; Seto, C. T.; Chin, D. N.; Mammen, M.; Gordon, D. M. *Acc. Chem. Res.* **1995**, *28*, 37.

Scheme 4. Self-Assembly of dppp-Chelated, Pt and Pd Macrocyclic Molecular Squares

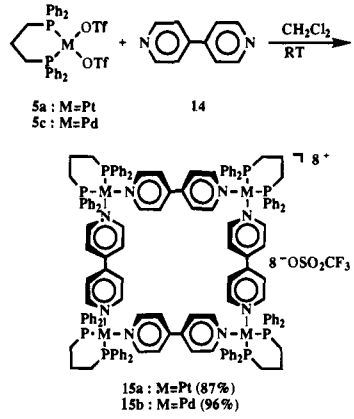

Scheme 5. Self-Assembly of Et_3P-Chelated, Pt and Pd Macrocyclic, Cationic Molecular Squares

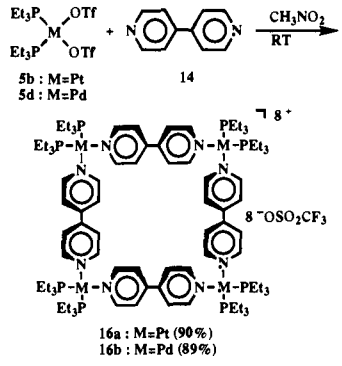

Formation of Cationic, Tetranuclear, Macrocyclic Squares. Chemists increasingly recognize the value of noncovalent interactions and the concomitant biology-based self-assembling processes and derived noncovalent synthesis.[22] Likewise, transition metal complexes generally have well-defined, specific geometries and coordination numbers and, when combined with di- and polydentate ligands with proper donor atoms in a desired spatial orientation, may lead via self-assembly to molecules with unique, specific shapes. Pt(II) and Pd(II) complexes are known to be tetracoordinated, square-planar species with ~90° bond angles around the metal center capable of both *cis* and *trans* geometry. Coordination with a diphosphine such as dppp results in a cyclic chelated complex, as in **5**, with a constrained *cis* geometry and hence two *adjacent* coordination sites occupied by weakly coordinating ligands that, when interacted with a bidentate ligand such as bipyridine, is precoded for self-assembly into a tetranuclear, macrocyclic molecular square.

Indeed, reaction of bis(triflate) complexes **5a,c** with an equimolar amount of 4,4′-bipyridine (**14**) at room temperature in CH_2Cl_2 results in the formation of the desired molecular squares, **15**, in a matter of minutes in excellent isolated yields (Scheme 4). Next we wished to determine if a cyclic bis(phosphine) complex is necessary to hold the desired *cis* geometry required for the self-assembly into molecular squares.

Interaction of the acyclic bis(triethylphosphine) *cis* complexes **5b,d**, respectively, with 1 equiv of bipyridine in CH_3NO_2 at room temperature likewise resulted in the desired molecular squares, **16** (Scheme 5), in excellent isolated yields, thereby ipso facto establishing that a cyclic bis(phosphine) to rigidly maintain the necessary *cis* geometry for self-assembly is not required.

Since it is known that bipyridine, like biphenyl, is not planar, but rather twisted by ~30−35° around the central C−C bond, we were interested in assembling a square with a planar

Scheme 6. Self-Assembly of Diazapyrene-Chelated, Pt and Pd Macrocyclic, Cationic Molecular Squares

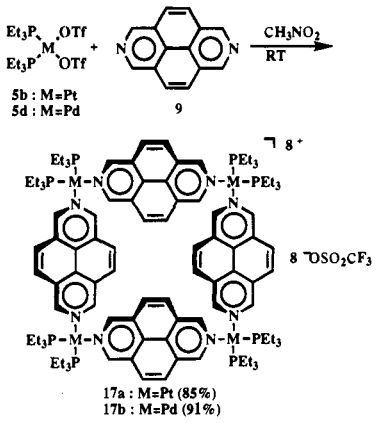

Scheme 7. Self-Assembly of Diazaperylene-Chelated, Tetranuclear, Cationic Molecular Squares

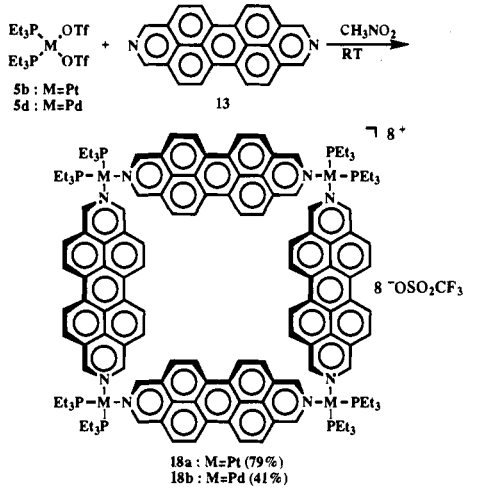

bidentate ligand such as 2,7-diazapyrene (**9**). Moreover, this ligand also adds depth to the resulting molecular square.

Interaction of the precursor triflate complexes **5b,d** with 1 equiv of diazapyrene **9** in CH_3NO_2 at room temperature gave the desired molecular squares, **17**, in high isolated yields (Scheme 6).

In order to prepare tetranuclear, macrocyclic molecular squares of differing sizes, we next examined the reactions of diazaperylene **13** and pyrazine **19** with the chelated precursor complexes **5**. Reaction of **5b,d** with an equimolar amount of diazaperylene **13** in CH_3NO_2 resulted in the desired molecular squares, **18** (Scheme 7), albeit in lower yields and impure. Interestingly, these self-assembled molecular squares, **18**, were more soluble in CH_3NO_2 than the precursor diazaperylene, **13**. Nevertheless, complete purification and full characterization of these large squares proved to be impossible because of their low solubility in all common organic solvents.

In contrast to the above-described reactions, all of which resulted in macrocyclic squares, the interaction of pyrazine (**19**) with **5**, regardless of stoichiometry, resulted in the formation of only the respective monomers, **20** (Scheme 8), as illustrated for **5a,c**.

The single crystal X-ray structures of **20** (vide infra) readily reveal the reason for the inability of **5** and **19** to self-assemble into the desired molecular square and the formation of only monometallic complexes **20**. The phenyl groups of the chelating dppp ligand are directly above the pyrazine rings in **20**, as seen from the respective ORTEPS, making it sterically impossible to bring in a second metal unit, **5**, as the respective phenyl

Scheme 8. Formation of Square-Planar Bis(pyrazine) Pt and Pd Complexes

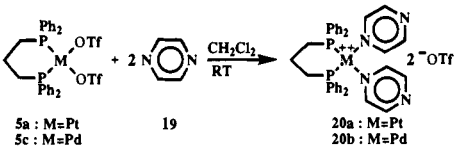

Scheme 9. Self-Assembly of Dicyano-Based Molecular Squares

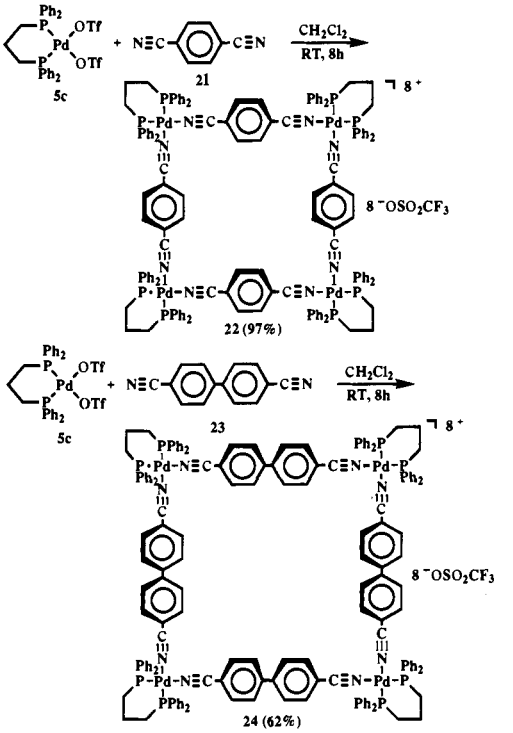

groups of the chelating phosphine on the adjacent metals would be in each other's way. Although the triethylphosphine groups of **5b,d** have a smaller cone angle and size than the phenyls of dppp, molecular models indicate that steric interaction still prevents the formation of the tetrameric molecular squares.

To date, all known,[13-17] charged, tetranuclear molecular squares have nitrogen-containing heteroaromatic bidentate ligands, such as bipyridine, as the central chelating units holding the assembly together. It was therefore of interest to examine other bidentate ligands such as cyano groups as possible chelating agents whose complexation with **5** might also result in molecular squares via self-assembly. Hence, we decided to investigate 1,4-dicyanobenzene (**21**) and 4,4′-dicyanobiphenyl (**23**) as possible chelating bidentate ligands for the formation of molecular squares.

Reaction of **5c** with equimolar amounts of **21** and **23** in CH_2Cl_2 at room temperature gave the corresponding macrocyclic molecular squares, **22** and **24**, respectively, as shown in Scheme 9.

Interestingly, the analogous Pt complex, **5a**, gave only oligomeric products upon reaction with either **21** or **23**, with no evidence for formation of the macrocyclic squares related to **22** and **24**. At the present time, we do not understand why Pd results in a macrocycle and Pt in only oligomers. Moreover, reaction of 2 equiv of the Pd complex, **5c**, with either **21** or **23** gave the corresponding dimetallic complexes, **25** and **26**, as stable isolable compounds (Scheme 10).

Despite the anti orientation of **25** (vide infra), reaction of preisolated **25** with an additional equivalent of **21** readily converts it into the tetranuclear, macrocyclic square, **22**.

Scheme 10. Formation of Bimetallic Dicyano Complexes **25** and **26**

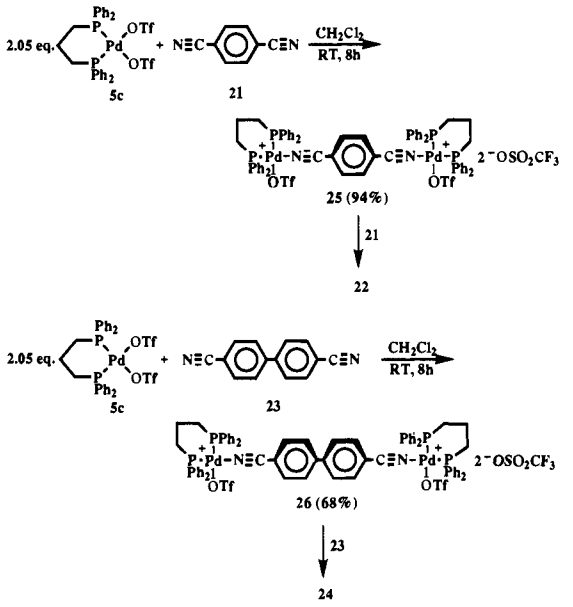

Likewise, reaction of preisolated[23] **26** with **23** results in **24**. However, attempts to prepare a molecular rectangle by reaction of either **25** with **23** or **26** with **21** results in a mixture of the two macrocyclic molecular squares, **22** and **24**, although small amounts of the rectangle may have escaped detection.

Properties and Characterization of Tetranuclear, Macrocyclic Squares and Related Species. All cationic, tetranuclear, macrocyclic squares isolated to date are robust, air-stable, microcrystalline solids. Compounds **15**, **16**, and **20a** are white or off-white in color, whereas **17**, **20b**, **22**, **24**, **25**, and **26** are yellow or bright yellow, and compounds **18a**,**b** are dark red.

All molecular squares decompose at their melting points, which are generally above 200 °C. All molecular squares described crystallize with either solvent or water of crystallization that generally cannot be driven off by heating in a vacuum. These molecules, despite their size and multiple charges, are remarkably soluble, with the exception of **18**, in many common organic solvents. The dppp-chelated species **15**, **22**, and **24** are soluble in CH_2Cl_2, $CHCl_3$, CH_3NO_2, acetone, ethanol, and methanol, whereas the Et_3P-chelated species are not as soluble in CH_2Cl_2 and $CHCl_3$ but dissolve in CH_3NO_2, CH_3CN, CH_3OH, and related polar solvents. All are insoluble in less polar solvents like pentane, hexane, benzene, ether, and toluene as well as water.

These unique macrocyclic squares are characterized by analytical and spectral means as detailed in the Experimental Section and, in the case of **15a**, by a single crystal X-ray determination. Specifically, all new compounds have elemental analyses consistent with their respective compositions. Multinuclear NMR, along with internal consistency in the spectral data among the diverse molecular squares, anchored to an X-ray determination unambiguously establishes their structures. In particular, the presence of the triflate counterion in all cases is indicated by both the infrared absorptions around 1160, 1100, and 1030 cm^{-1} and the ^{19}F signal at about −78 ppm highly characteristic of ionic triflates.[24] In accord with the high symmetry of these molecular squares, all $^{31}P\{^1H\}$ spectra display sharp singlets, with appropriate Pt satellites in the case of the Pt complexes, as predicted for the eight equivalent chelating phosphorus groups. Moreover, in all cases the ^{31}P signals are shifted by several ppm, as expected, upon further complexing in the molecular squares relative to the precursor square-planar metal complexes, **5**.

Especially diagnostic for the structure of these macrocyclic, tetranuclear squares are the respective ^1H and $^{13}C\{^1H\}$ NMR signals. In all molecular squares, the proton signals of the chelating phosphine units (i.e., the methylene protons of dppp and the ethyl signals of Et_3P) are shifted downfield, as expected for these cationic species, relative to the same signals in the neutral precursors, **5**. Most importantly, the coordinated 4,4′-bipyridine ligands in **15** and **16** as well as the diazapyrene ligands in **17** display only two signals in the ^1H NMR, as required for these symmetrical molecules. Moreover, the protons α to the chelating nitrogen are significantly downfield shifted (by 0.3−0.6 ppm) upon complexing relative to those of the uncoordinated starting 4,4′-bipyridine (**14**) and the diazapyrene **9**. Likewise, H_β in **16** and the H_γ in **17** are downfield shifted relative to those of the free precursors **14** and **9**, albeit much less than H_α (by ~0.1 ppm) upon formation of the molecular squares. In contrast, H_β in **15** are upfield shifted by ~0.6 ppm compared to those of the uncoordinated **14**. This unusual upfield shift is due to the shielding provided by the dppp phenyl rings that sit over the bipyridine unit (see ORTEP in Figure 1) in these macrocyclic systems. Evidence for this hypothesis is provided by the expected observation of a downfield shift of these same H_β proton signals in **16** where the phenyls of **15** are replaced by ethyl groups.

Finally, all ^{13}C spectral signals are consistent with the proposed structures and internally consistent with each other among the related macrocyclic squares.

Single Crystal X-ray Molecular Structure Determinations. As these molecular squares represent unique, interesting substances, their exact structures are of considerable interest. Hence, we attempted to obtain single crystals and carry out X-ray molecular structure determinations of all macrocyclic squares described above. Unfortunately, to date we have only obtained suitable crystals for **15a**. However, we were also able to obtain appropriate crystals and structures for **20a**,**b** as well as **25**, a precursor to square **22**. Crystallographic data for **15a**, **20a**,**b**, and **25** are summarized in Table 1, and numbering diagrams, ORTEP representations, and important geometric features are shown in Figures 1−4. Important interatomic bond distances and angles are given in Tables 2−4.

Perusal of the crystallographic data reveals a number of interesting structural features. The coordination geometry about the cationic Pt(II) and Pd(II) metal centers is normal square-planar, with slight deviations of the angles. All M−P distances are normal, with a range of 2.22−2.28 Å. Likewise, the M−N distances are normal, with a range of 2.04−2.13 Å.

Not surprisingly, the molecular structures of the Pt and Pd bis(pyrazine) complexes **20** are very similar. The N−Pt−N angle of 87° in the Pt complex **20a** is a bit larger than the analogous N−Pd−N angle of 85.6° in **20b**. The unique feature of these complexes is the position of one of the dppp phenyls nearly parallel with and on top of the chelated pyrazine unit.

Likewise, the bis-metallic complex **25** is square-planar around the Pd centers. The Pd−Pd distance in this complex is 12.2 Å. Hence, the cavity size of molecular square **22** is about 10% larger (Pd−Pd of 12.2 Å in **22** vs Pt−Pt of 11.2 Å in **15a**) than that of Pt-bipy tetramer **15a**. The noteworthy feature of this molecular structure is the anti arrangement of the two Pd-bound triflate units. Despite this anti orientation of the labile triflate ligands, further reaction of **22** with 1 equiv of 1,4-dicyanobenzene produces the molecular square **22** rather than an oligomer.

(23) We do not know the geometry of **26**, as to date we have not been able to obtain an X-ray quality crystal.

(24) Lawrence, G. A. *Chem. Rev.* **1986**, *86*, 17 and references cited therein.

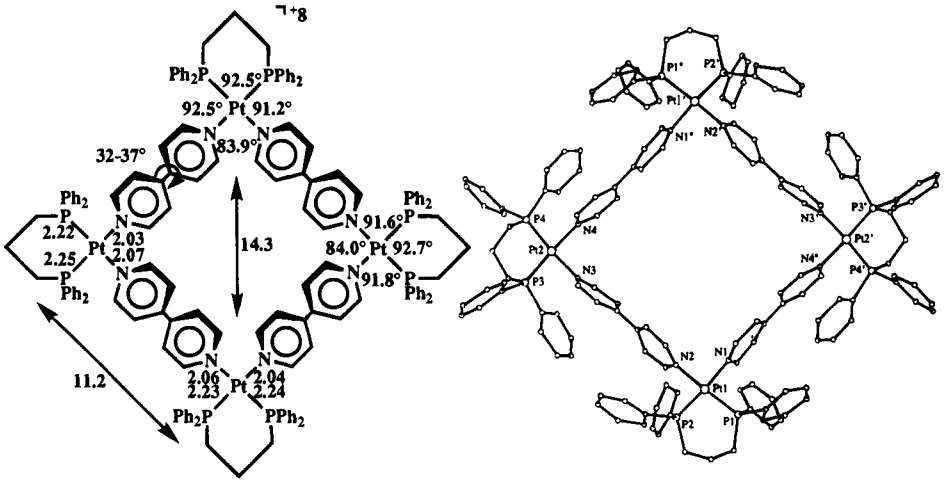

Figure 1. ORTEP representation and summary of the significant geometric features of the cationic portion of molecular square **15a**.

Table 1. Crystallographic Data for **15a**, **20a**, **20b**, and **25**

	15a	**20a**	**20b**	**25**
molecular formula	$Pt_4C_{156}H_{136}N_8P_8S_8O_{24}F_{24}$	$PtC_{38}H_{36}N_4P_2S_2O_6F_6Cl_2$	$PdC_{38}H_{36}N_4P_2S_2O_6F_6Cl_2$	$Pd_2C_{66}H_{56}N_2P_4S_4O_{12}F_{12}$
fw, g mol^{-1}	4247.5	1150.8	1062.1	1762.1
space group	$P2/n$	$P2_1/m$	$P2_1/c$	$P2_1/c$
space group no.	13.0	11.0	14.0	14.0
crystal system	monoclinic	monoclinic	monoclinic	monoclinic
a, Å	22.833(6)	11.116(2)	20.529(5)	9.862(1)
b, Å	15.869(4)	14.563(2)	11.529(4)	17.137(1)
c, Å	34.192(9)	13.921(2)	21.257(5)	21.018(2)
β, deg	100.35(2)	98.67(2)	118.13(2)	101.77(1)
V, Å^3	12 187.71	2227.59	4437.21	3477.45
Z	2.0	2.0	4.0	2.0
D_{calc}, g cm^{-3}	1.157	1.716	1.590	1.683
crystal size	0.30 × 0.23 × 0.15	0.25 × 0.20 × 0.15	0.28 × 0.25 × 0.23	0.45 × 0.40 × 0.32
absorption coeff, cm^{-1}	24.924	35.347	7.666	8.074
radiation	Mo (0.709 30 Å)	Mo (0.709 30 Å)	Mo (0.709 30 Å)	Mo (0.710 73 Å)
no. of reflcns measd	18 098	4310	7778	6898
no. of unique reflcns	16 864	4089	7121	6124
no. of reflcns obsd	7039 ($I < 3.20\sigma(I)$)	3666 ($I < 3.0\sigma(I)$)	4212 ($I < 3.0\sigma(I)$)	5183 ($I < 3.0\sigma(I)$)
2θ range, deg	2−48	4−50	4−48	3−48
scan technique	$\theta/2\theta$	$\theta/2\theta$	$\theta/2\theta$	$\theta/2\theta$
scan width, deg	0.80 + 0.340 tan θ	0.80 + 0.340 tan θ	0.80 + 0.340 tan θ	$K_{\alpha1}(1.2) - K_{\alpha2} - 1.2$
goodness-of-fit	2.689	1.211	3.746	1.590
R	0.0888	0.0289	0.0572	0.0284
R_w	0.1158	0.0332	0.0637	0.0494

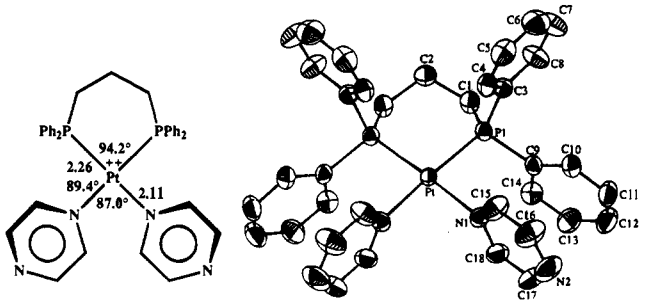

Figure 2. ORTEP diagram and summary of important bond lengths and bond angles of the cationic portion of complex **20a**.

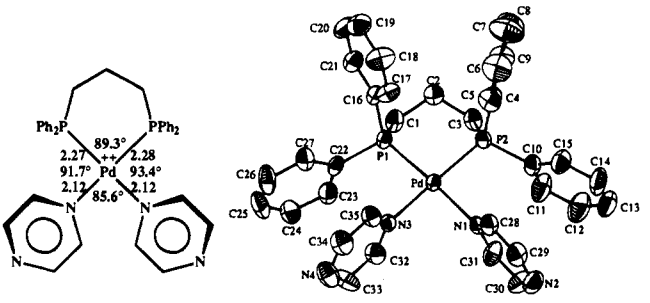

Figure 3. ORTEP representation and summary of important bond lengths and bond angles of the cationic portion of complex **20b**.

Obviously the most interesting structure is that of **15a**. The X-ray structural data clearly show four dppp-chelated Pt(II) units which occupy the corners of a square, held together by chelating 4,4′-bipyridine groups. The edge-to-edge Pt−Pt distance is 11.2 Å, and the diagonal Pt−Pt distance is nearly 15 Å. In order to accommodate the N−Pt−N angles of 84° and 83.9° (rather than the ideal square-planar angles of 90°), the molecule is "puckered", as shown in Figure 5. In other words, although the molecule's shape is indeed that of a square, it is not planar, the deviation from planarity being about 4 Å. Moreover, the 4,4′-bipyridyl units are not planar but are twisted about the central C−C bond by 32−37°.

Particularly interesting is the stacking pattern in the solid state, as shown in Figure 6. The cationic squares are stacked along the b-axis, resulting in long channel-like cavities (see Figure 6). The repeating units are 15.9 Å apart. Because a couple of the triflate counterions were disordered, and also due to solvent occlusion and the general complexity of the structure, we were unable to refine the molecular structure to better than $R = 8.9$ and fully locate all the triflate counterions. Nevertheless, the

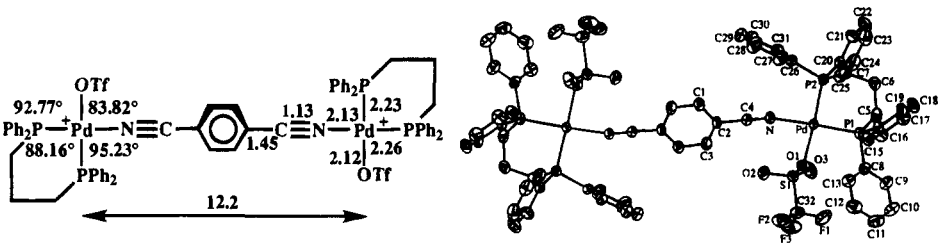

Figure 4. ORTEP diagram and summary of the significant geometric features of the cationic portion of complex **25**.

Table 2. Relevant Bond Distances (Å) and Angles (Deg) for Molecular Square **15a**

Pt(1)–Pt(1′)	14.299(2)	N(1)–Pt(1)–N(2)	83.9(8)
Pt(1)–Pt(2)	11.225(4)	N(3)–Pt(2)–N(4)	84.0(9)
Pt(1)–N(1)	2.04(2)	P(1)–Pt(1)–N(1)	92.5(6)
Pt(1)–N(2)	2.06(2)	P(2)–Pt(1)–N(2)	91.2(6)
Pt(2)–N(3)	2.07(2)	P(3)–Pt(2)–N(3)	91.6(6)
Pt(2)–N(4)	2.03(2)	P(4)–Pt(2)–N(4)	91.8(7)
Pt(1)–P(1)	2.235(8)	P(1)–Pt(1)–P(2)	92.5(3)
Pt(1)–P(2)	2.228(8)	P(3)–Pt(2)–P(4)	92.7(3)
Pt(2)–P(3)	2.249(7)	P(1)–Pt(1)–N(2)	175.9(7)
Pt(2)–P(4)	2.224(7)	P(2)–Pt(1)–N(1)	175.0(6)
		P(3)–Pt(2)–N(4)	175.5(7)
		P(4)–Pt(2)–N(3)	175.7(6)

Table 3. Relevant Bond Distances (Å) and Angles (Deg) for Complexes **20a** and **20b**

		20a	
Pt–N(1)	2.109(4)	N(1)–Pt–N(1′)	87.0(2)
Pt–P(1)	2.262(1)	P(1)–Pt–P(1′)	94.2(1)
		P(1)–Pt–N(1)	89.4(1)
		P(1)–Pt–N(1′)	176.4(1)
		20b	
Pd–N(1)	2.115(4)	N(1)–Pd–N(3)	85.6(1)
Pd–N(3)	2.121(4)	N(1)–Pd–P(2)	93.4(1)
Pd–P(1)	2.273(1)	N(3)–Pd–P(1)	91.7(1)
Pd–P(2)	2.284(1)	P(1)–Pd–P(2)	89.31(4)
		N(1)–Pd–P(1)	176.8(1)
		N(3)–Pd–P(2)	178.8(1)

Table 4. Relevant Bond Distances (Å) and Angles (Deg) for Complex **25**

Pd–N	2.131(2)	N–Pd–O(1)	83.82(7)
Pd–P(1)	2.2600(5)	N–Pd–P(2)	95.23(5)
Pd–P(2)	2.2252(6)	P(1)–Pd–P(2)	88.16(2)
Pd–O(1)	2.118(2)	P(1)–Pd–O(1)	92.77(5)
N–C(4)	1.131(3)	N–Pd–P(1)	176.38(5)
C(2)–C(4)	1.453(3)	P(2)–Pd–O(1)	178.40(5)
		Pd–N–C(4)	167.3(2)
		N–C(4)–C(2)	178.9(3)

data show that the triflates are stacked below and above (rather than inside the cavity) of an individual molecular square.

It is interesting to compare and contrast the structure of molecular square **15a** with that of the only other known[13,25] molecular structure of a related species, **26** (Figure 7). The Pt–N–uracyl bond length of 2.03 Å compares favorably with the Pt–N–bipy bond length of 2.05 Å in **15a**, despite a chelating ethylenediamine in **26** instead of the chelating dppp unit in our **15a**. In contrast, the N–Pt–N interatomic angle of 89.5° in **26** is considerably larger and results in less distortion of the square than the comparable N–Pt–N bond angles of 84–85° in **15a**. This difference is likely due to the need for a larger P–Pt–P angle for the chelating dppp unit in **15a** (92.5–92.7°), compared to the smaller N–Pt–N angle of 85° for the chelating ethylenediamine of **26**. Due to chelation by uracyls rather than bipy, the edge-to-edge Pt–Pt distance in **26** is only 5.86 Å,

(25) Rauter, H.; Hillgeris, E. C.; Lippert, B. *J. Chem. Soc., Chem. Commun.* **1992**, 1385.

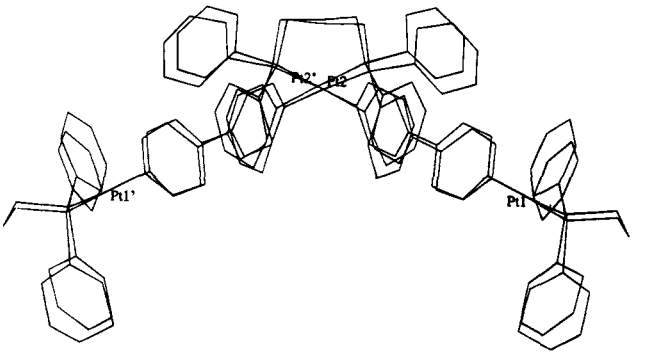

Figure 5. Side view of molecular square **15a**, displaying the "puckered" geometry.

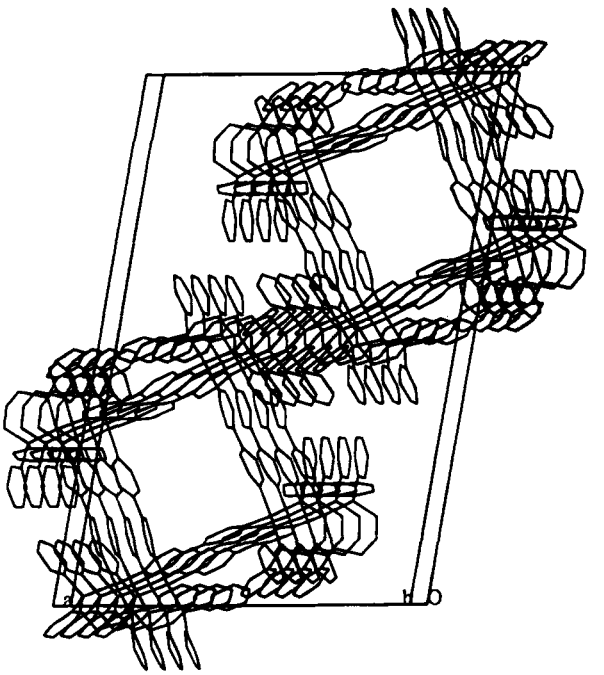

Figure 6. Packing of the cationic portion of molecular square **15a**. The view is along the *b*-axis.

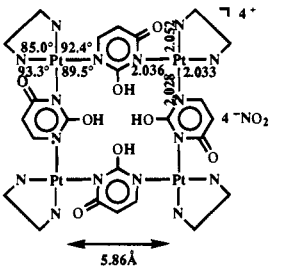

Figure 7. Molecular structure of tetranuclear complex **26**.[13]

compared to 11.2 Å in our **15a**, with, of course, a concomitantly smaller cavity and channel in **26** vs **15a**.

Our assumption is that the remaining molecular squares, in particular **15b**, **16a,b**, and likely **17a,b**, are similar in structure

to **15a**, at least in their gross geometric features. We are continuing to attempt to grow suitable single crystals for X-ray structure determination of all the above-described molecular squares.

Chemistry of Molecular Squares. To date we have concentrated our efforts on the assembly, characterization, and structure of these unique molecules. We were particularly interested in scoping the diverse bifunctional ligand systems (**9**, **13**, **14**, **19**, **21**, and **23**) that might self-assemble into molecular squares with the variously chelated metal precursors **5**.

Clearly these novel macrocyclic systems are potentially well suited for host–guest chemistry, catalyses, noncovalent interactions, etc. Herein we report preliminary observations on the chemistry and in particular some host–guest interactions with our molecular squares.

To assess the solution stability of these macrocyclic molecular squares, the ^{1}H NMR of compound **17a** in CD_3NO_2 was examined between the temperatures of −20 and +90 °C. No change in the ^{1}H NMR was observed in this 110 °C temperature range.

It is known that C≡N groups form considerably weaker complexes with Pt and Pd than pyridine. Therefore, we examined the behavior of molecular square **22** in the presence of 4 equiv of bipy (**14**). Interestingly, complete and clean conversion of **22** to the bipy-based molecular square **15a** occurred in CD_2Cl_2 at room temperature, along with liberation of free NCC_6H_4CN (**21**) in a matter of minutes. Likewise, reaction of the dinuclear complex **25** with **14** in CD_2Cl_2 gave the macrocyclic square **15b**. In contrast, as expected, no change was observed upon the addition of 4 equiv or excess of 1,4-dicyanobenzene (**21**) to molecular square **15b**. These data indicate that the CN-based molecular squares **22** and **24** are rather fluxional and less stable in solution than the bipy-chelated macrocycles.

The majority of currently known host–guest interactions involve cation (usually metals) guests. By virtue of the high positive charges (8+) in these macrocyclic molecular squares, they should be effective hosts for electron-rich species. Based upon the size (M–M distance of ~11 Å) of these macrocyclic systems, we chose to examine the host–guest interactions between three representative squares, **15a,b** and **17a**, and an electron-rich guest, 1,5-dihydroxynaphthalene (**27**). As the para

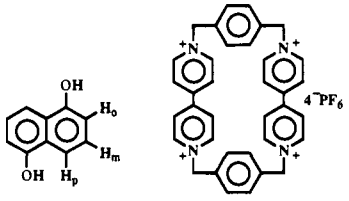

27 28

protons of guest **27** were obscured by the aromatic signals due to the host molecules **15a,b**, the chemical shifts of the ortho and meta protons were followed as a function of the increasing concentration of the hosts in CD_3OD at room temperature. A typical plot of the *change* in chemical shifts (*all upfield* shifts) in ppm of the ortho and meta protons of **27** as a function of the concentration of host **15a** is given in Figure 8. Solubility did not allow host–guest concentrations beyond 3.5:1.0. As seen from this plot, there is a significant upfield shift, ~0.11 ppm for the ortho and ~0.2 ppm for the meta signals, as a function of concentration. At a host–guest concentration of 3.5:1.0, the shift of the ortho protons of **27** has nearly leveled off, whereas the leveling has not yet been fully reached for the meta protons of **27** at this concentration. Essentially identical results were

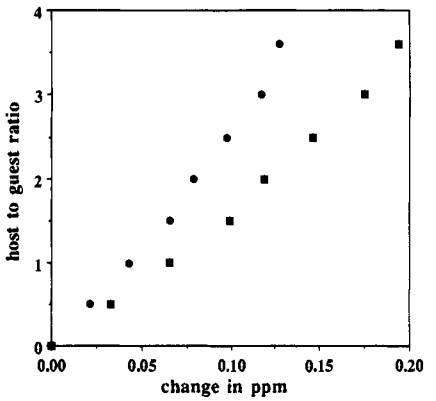

Figure 8. Plot of change in chemical shifts of the ortho (●) and meta (■) protons as a function of concentration of host **15a**.

obtained for the Pd analog **15b** with **27**, and very similar results were seen for **17a** with **27** (data are given in Table 5, below). Unfortunately, solubility limitations allowed a host–guest ratio of only 2.5:1.0 for these latter two macrocyclic molecular squares, and hence the leveling effect expected for these interactions was not observable in these two systems.

These data definitely demonstrate the formation of inclusion complexes between our macrocyclic molecular squares and an electron-rich guest **27**. Both the magnitude and the directions of these chemical shifts are comparable to those observed by Stoddart and co-workers[26] with the cationic cyclophane host **28** and guest **27**.

Conclusions

A new class of compounds, cationic, tetranuclear, Pt(II)- and Pd(II)-based macrocyclic squares, can be readily formed in high isolated yields via self-assembly using a variety of difunctional chelating ligands, such as bipyridine, dicyanobenzene, and the square-planar *cis*-bis(phosphine) Pt and Pd bis(triflate) complexes. Due to the *cis* geometry and the concomitant two adjacent coordination sites occupied by the weakly coordinating triflate ligands at an interatomic TfO–M–OTf angle of ~90°, these complexes are preprogrammed for self-assembly with appropriate bidentate ligands into unique macrocyclic molecular squares. In spite of the large positive charge (8+) as well as high molecular weights (>4000) of these molecular squares, they are remarkably soluble in many organic solvents. The X-ray crystal structure establishes the dimension of the bipy and related squares to be just over 11 Å on the sides, based on the M–M interatomic distances. The stacking diagram shows a channel in the solid state.

These novel metal-based molecular squares represent new materials with as yet unexplored unique properties. Uses envisioned for these molecules include inclusion phenomena, catalyses, host–guest interactions with electron-rich and anionic guests, noncovalent interactions, and ultimately perhaps nanoscale molecular devices. Indeed, concentration-dependent upfield chemical shifts are observed for the ortho and meta protons of 1,5-dihydroxynaphthalene in the presence of molecular squares **15a,b** and **17a**, indicating noncovalent host–guest interactions and inclusion phenomena.

The preparation of other molecular squares and rectangles via complete or modular self-assembly and the properties and chemistry of these unique macrocycles are the subject of

(26) Annelli, P. L.; Ashton, P. R.; Ballardini, R.; Balzani, V.; Delgado, M.; Gandolfi, M. T.; Goodnow, T. T.; Kaifer, A. E.; Philip, D.; Pietraszkiewicz, M.; Prodi, L.; Reddington, M. V.; Slawin, A. M. Z.; Spencer, N.; Stoddart, J. F.; Vincent, C.; Williams, D. J. *J. Am. Chem. Soc.* **1992**, *114*, 193. Annelli, P. L.; Ashton, P. R.; Spencer, N.; Slawin, A. M. Z.; Stoddart, J. F.; Williams, D. J. *Angew. Chem., Int. Ed. Engl.* **1991**, *30*, 1036.

ongoing studies and will be reported in future papers as they are uncovered.

Experimental Section

General Methods. All reactions were conducted under a dry nitrogen atmosphere using Schlenk techniques, unless otherwise noted. IR spectra were recorded on a Mattson Polaris FT-IR spectrophotometer. NMR spectra were recorded on a Varian XL-300 or a Unity-300 spectrometer. ^{1}H NMR spectra were recorded at 300 MHz, and all chemical shifts (δ) are reported in ppm relative to tetramethylsilane (Me_4Si) as an internal standard or the proton resonance resulting from incomplete deuteration of the NMR solvent: $CDCl_3$ (7.24 ppm), C_6D_6 (7.15 ppm), CD_2Cl_2 (5.32 ppm), or CD_3NO_2 (4.33 ppm). ^{13}C NMR spectra were recorded at 75 MHz, and all chemical shifts are reported in ppm relative to the carbon resonance of the deuterated NMR solvent: $CDCl_3$ (77.0 ppm), CD_3NO_2 (62.8 ppm), or CD_2Cl_2 (53.8 ppm). ^{31}P NMR spectra were recorded at 121 MHz, and all chemical shifts are reported in ppm relative to external 85% H_3PO_4 at 0.00 ppm. ^{19}F NMR spectra were recorded at 282 MHz, and all chemical shifts are reported relative to external $CFCl_3$ at 0.00 ppm. Microanalyses were performed by Atlantic Microlab Inc., Norcross, GA. Melting points were obtained with a Mel-Temp capillary melting point apparatus and were not corrected.

Materials. Solvents were purified as follows. CH_3NO_2, CH_2Cl_2, $CHCl_3$, C_6H_6, $PhCH_3$, and hexanes were purified according to literature procedures[27] and were distilled over CaH_2. Ether and THF were purified according to literature procedures[27] and were distilled over Na/benzophenone. CH_3CN and CD_3NO_2 were distilled over CaH_2. $CDCl_3$, CD_2Cl_2, and C_6D_6 were vacuum transferred from CaH_2. All solvents were freeze−thaw−pump degassed three times before use.

All commercial reagents were ACS reagent grade and were obtained as follows: 4,4′-bipyridine (Aldrich), 1,4-dicyanobenzene (Aldrich), 4,4′-dicyanobiphenyl (Lancaster), 1,4,5,8-naphthalenetetracarboxylic dianhydride (Aldrich), 40% aqueous methylamine (Lancaster), aluminum chloride (Fisher Scientific), lithium aluminum hydride (Aldrich), 10% Pd/C (Janssen Chimica), $(C_6H_5)_2P(CH_2)_3P(C_6H_5)_2$ (dppp) (Aldrich), $PtCl_2$ (Strem), $PdCl_2$ (Strem), K_2PtCl_4 (Aldrich), and K_2PdCl_4 (Strem) were all used as received; silver trifluoromethanesulfonate,[28] *cis*-Pt(dppp)$(Cl)_2$,[19] *cis*-Pd(dppp)$(Cl)_2$,[19] *cis*-Pt$(PEt_3)_2(Cl)_2$,[18] *cis*-Pd$(PEt_3)_2(Cl)_2$,[18] 2,7-diazapyrene,[20] and 2,9-diazadibenzo[*cd,lm*]perylene[21] were prepared according to modified literature procedures.

Preparation of Pt(dppp)$(OTf)_2$ (5a). To a solution in a Schlenk flask containing 710 mg (1.04 mmol) of Pt(dppp)$(Cl)_2$ in 60 mL of CH_2Cl_2 was added 2.14 g (8.35 mmol) of AgOTf. The reaction mixture was stirred at 25 °C for 72 h with the exclusion of light. The heterogeneous mixture was filtered and concentrated to 10 mL under reduced pressure, followed by the addition of diethyl ether to precipitate the halogen-exchanged metal triflate complex. Collection and drying under vacuum in a drying tube gave an off-white solid, 925 mg (98%) of **5a**: mp 148−150 °C dec; IR (CCl_4) 3043, 2962, 1290, 1170, 1102, 1031 cm^{-1}; ^{31}P NMR (CD_2Cl_2) δ −6.9 (J_{Pt-P} = 3726 Hz); ^{19}F NMR (CD_2Cl_2) δ −77; ^{1}H NMR (CD_2Cl_2) δ 7.6−7.4 (m, 20H), 2.7 (m, 4H), 2.2 (m, 2H); ^{13}C NMR (CD_2Cl_2) δ 133.4 (C_o), 133.2 (C_p), 129.2 (C_m), 123.6 (C_{ipso}), 120.0 (q, OTf, J_{C-F} = 317 Hz), 23.5 ($P(CH_2)_2$), 18.7 (CH_2).

Preparation of *cis*-Pt$(PEt_3)_2(OTf)_2$ (5b). To a Schlenk flask containing 960 mg (1.91 mmol) of Pt$(PEt_3)_2(Cl)_2$ in 70 mL of CH_2Cl_2 was added 1.23 g (4.78 mmol) of AgOTf. The reaction mixture was allowed to stir at 25 °C for 12 h with the exclusion of light. The heterogeneous mixture was filtered and concentrated to 15 mL under reduced pressure, followed by the addition of diethyl ether to precipitate the metal triflate complex. Collection and drying under vacuum in a drying tube gave an analytically pure, white powder, 1.26 (90%) of **5b**: mp 224−227 °C dec; IR (CCl_4) 2973, 2939, 1302, 1227, 1206, 1171, 1022 cm^{-1}; ^{31}P NMR (CD_3NO_2) δ 16 (J_{Pt-P} = 3814 Hz); ^{19}F NMR (CD_3NO_2) δ −76; ^{1}H NMR (CD_3NO_2) δ 2.1 (m, CH_2), 1.3 (m, CH_3); ^{13}C NMR (CD_3NO_2) δ 121 (q, OTf, J_{C-F} = 317 Hz), 16.2 (CH_2), 8.5 (CH_3). Anal. Calcd for $C_{14}H_{30}PtP_2S_2O_6F_6{\cdot}2H_2O$: C, 21.96; H, 4.48; S, 8.38. Found: C, 22.05; H, 4.38; S, 7.84.

(27) Perrin, D. D.; Armarego, W. L. F. *Purification of Laboratory Chemicals*; Pergamon Press: Oxford, 1988.

(28) Gramstad, T.; Haszeldine, R. N. *J. Chem. Soc.* **1957**, 2640. Modification of this procedure involves a nonaqueous preparation of silver triflate using a 1:1 ether and toluene mixture as solvent instead of H_2O.

Preparation of Pd(dppp)$(OTf)_2$ (5c). In analogy with the preparation of **5a**, 122 mg (0.207 mmol) of Pd(dppp)$(Cl)_2$ was reacted with 159 mg (0.621 mmol) of AgOTf in 20 mL of CH_2Cl_2 for 12 h at 25 °C. A similar workup resulted in the formation of an analytically pure, yellow powder, 155 mg (92%) of **5c**: mp 189−190 °C dec; IR (CCl_4) 3062, 2920, 1274, 1168, 1098, 1019 cm^{-1}; ^{31}P NMR (CD_2Cl_2) δ 20.0; ^{19}F NMR (CD_2Cl_2) δ −76; ^{1}H NMR (CD_2Cl_2) δ 7.6−7.4 (m, 20H), 2.7 (m, 4H), 2.3 (m, 2H); ^{13}C NMR (CD_2Cl_2) δ 133.6 (C_o), 133.3 (C_p), 129.7 (C_m), 123.9 (C_{ipso}), 120.2 (q, OTf, J_{C-F} = 317 Hz), 23.3 ($P(CH_2)_2$), 18.6 (CH_2).

Preparation of *cis*-Pd$(PEt_3)_2(OTf)_2$ (5d). In analogy with the preparation of **5b**, 202 mg (0.49 mmol) of Pd$(PEt_3)(Cl)_2$ was reacted with 314 mg (1.22 mmol) of AgOTf in 20 mL of CH_2Cl_2 for 3 h at 25 °C. A similar workup resulted in the formation of an analytically pure, bright yellow powder, 250 mg (80%) of **5d**: mp 173−176 °C; IR (CCl_4) 2966, 2918, 1293, 1227, 1169, 1026 cm^{-1}; ^{31}P NMR (CD_3NO_2) δ 56; ^{19}F NMR (CD_3NO_2) δ −76; ^{1}H NMR (CD_3NO_2) δ 2.1 (m, CH_2), 1.3 (m, CH_3); ^{13}C NMR (CD_3NO_2) δ 122 (q, OTf, J_{C-F} = 317 Hz), 17.6 (CH_2), 8.7 (CH_3). Anal. Calcd for $C_{14}H_{30}PdP_2S_2O_6F_6{\cdot}2H_2O$: C, 24.84; H, 5.06; S, 9.47. Found: C, 24.87; H, 4.98; S, 9.14.

Preparation of 2,7-Diazapyrene (9). A three-neck flask equipped with a mechanical stirrer and a reflux condenser was charged with 800 mL of 40% aqueous methylamine. To the solution was added slowly 25 g (93 mmol) of 1,4,5,8-naphthalenetetracarboxylic dianhydride. The suspension was refluxed for 3 h, cooled to 25 °C, collected by filtration, and washed with methanol to afford a pink powder, 26.6 g (90 mmol, 97%). IR and ^{1}H NMR showed that the product is identical with *N,N′*-dimethyl-1,4,5,8-naphthalenetetracarboxylic diimide.[20] The diimide was reduced according to literature procedure using $AlCl_3$−$LiAlH_4$ in THF[20] to give 1,3,6,8-tetrahydro-2,7-dimethyl-2,7-diazapyrene.

A mixture containing 12 g (50 mmol) of 1,3,6,8-tetrahydro-2,7-dimethyl-2,7-diazapyrene and 10 g of 10% Pd/C was heated in a sand bath under N_2 to 300−310 °C for 1 h. The mixture was cooled to 25 °C under the flow of N_2 and extracted with 400 mL of hot 1 N aqueous HCl, followed by basification and isolation of a brown residue. The crude product was purified by a combination of column chromatography (Al_2O_3, eluent 3% Et_3N−C_6H_6:CH_2Cl_2 5:1 → 1:1), recrystallization (C_6H_6), and sublimation (140 °C, 0.05 mmHg) to afford a yellow powder, 2.40 g (23%) of **9**: mp 284−287 °C (lit.[20] mp 283−284 °C); ^{1}H NMR (CD_3NO_2) δ 9.5 (s, 4H), 8.3 (s, 4H); ^{13}C NMR (CD_3NO_2) δ 146.5 (C_α), 127.7 (C_γ), 127.3 (C_{ipso}), 127.2 (C_β).

Preparation of *N,N′*-Dimethyl-3,4,9,10-perylenetetracarboxylic Diimide (11). A three-neck flask equipped with a mechanical stirrer and a reflux condenser was charged with 600 mL of 40% aqueous methylamine. To the solution was added slowly 3,4,9,10-perylenetetracarboxylic dianhydride (25 g, 64 mmol). The suspension was refluxed for 3 h and cooled to 25 °C. The red powder collected was washed with methanol and dried to afford 26.3 g (98%) of **11**: mp > 400 °C; IR (CCl_4) 1698, 1663, 1595, 1400, 1357, 1284, 1054 cm^{-1}; ^{1}H NMR (D_2SO_4; CD_2Cl_2 internal standard) δ 9.2 (m, 8H), 4.01 (s, 6H). Anal. Calcd for $C_{26}H_{14}N_2O_4{\cdot}0.5H_2O$: C, 73.06; H, 3.54; N, 6.54. Found: C, 73.28; H, 3.63; N, 6.61.

Preparation of 1,3,8,10-Tetrahydro-2,9-dimethyl-2,9-diazadibenzo[*cd,lm*]perylene (12). A three-neck flask equipped with a mechanical stirrer and a reflux condenser was charged with a solution of anhydrous $AlCl_3$ (143 mmol) in dry THF (500 mL). To the solution was added carefully $LiAlH_4$ (430 mmol) at 0 °C, followed by the addition of 25.4 g (61 mmol) of the crushed diimide. ***Caution!*** Addition of $LiAlH_4$ or the diimide is exothermic and may cause severe flothing. The dark blue suspension was heated carefully to reflux and maintained for 4 h. The suspension was then cooled to 25 °C and slowly added to 500 mL of ice water. The brown powder was extracted with refluxing $CHCl_3$ in a Soxhlet extractor (total required, 14 L). The extract was concentrated to ~50 mL under reduced pressure, and the brown powder formed was collected and dried to afford 12.0 g (54%) of **12**. The diamine was further purified by recrystallization from pyridine to give brown needles: mp 224−254 °C dec; IR (CCl_4) 2772, 1549, 1368, 1279, 1246, 1123 cm^{-1}; ^{1}H NMR (CF_3COOD; CD_2Cl_2 internal standard) δ 8.4 (d, 4H), 7.6 (d, 4H), 5.0 (dd, 4H), 4.7 (dd, 4H), 3.3 (s, 6H); ^{13}C NMR (CF_3COOD; CD_2Cl_2 internal standard) δ 133.4 (C_{ipso}), 129.5 ($C_{\gamma'}$), 127.9 ($C_{\delta'}$), 127.4 (C_γ), 124.4 (C_β), 122.9 (C_δ), 58.7 (CH_2), 43.7 (CH_3). Anal. Calcd for $C_{26}H_{22}N_2$: C, 86.15; H, 6.12; N, 7.73. Found: C, 86.24; H, 6.14; N, 7.69.

Preparation of 2,9-Diazadibenzo[*cd,lm*]perylene (13). A mixture containing 7 g (19 mmol) of diamine and 7 g of 10% Pd/C was heated in a sand bath under N_2 to 300−310 °C for 1 h. The mixture was cooled to 25 °C under the flow of N_2 and extracted with 400 mL of pyridine with a Soxhlet extractor for 72 h. The extract was reduced to 100 mL by rotary evaporation and cooled to −20 °C to afford a yellow powder (0.41 g). The remaining residue was then refluxed for an additional 96 h with 300 mL of pyridine, and the extract was treated in a similar manner to give a yellow powder (0.32 g); total 0.73 g (12%) of **13**. The crude product was further purified by recrystallization with pyridine to give golden yellow flakes: mp 328 °C dec; IR (CCl_4) 1586, 1550, 1535, 1394, 1381, 1240, 893 cm^{-1}; ^1H NMR (D_2SO_4) δ 9.74 (s, 4H), 9.63 (d, J = 9.5 Hz, 4H), 8.69 (d, J = 9.3 Hz, 4H); ^1H NMR (CF_3COOD; CD_2Cl_2 internal standard) δ 10.0 (d, J = 9.6 Hz, 4H), 9.9 (s, 4H), 9.1 (d, J = 9.3 Hz, 4H); ^{13}C NMR (CF_3COOD; CD_2Cl_2 internal standard) δ 136.2 (C_α), 132.6 (C_{ipso}), 131 ($C_{\gamma'}$), 130.2 (C_γ), 129.7 ($C_{\delta'}$), 128.2 (C_δ), 123.7 (C_β). Anal. Calcd for $C_{24}H_{12}N_2 \cdot 0.25H_2O$: C, 86.60; H, 3.78; N, 8.42. Found: C, 86.69; H, 3.83; N, 8.40.

Preparation of [Pt(4,4′-bipyridyl)(dppp)$_2$(OTf)$_2$]$_4$ (15a). To a 100 mL Schlenk flask, equipped with a stir bar, containing 212 mg (0.23 mmol) of **5a** in 50 mL of CH_2Cl_2 was added 37 mg (0.23 mmol) of 4,4′-bipyridine. The resulting homogeneous reaction mixture was stirred at 25 °C for 3 h. The reaction mixture was filtered through a coarse-porosity glass frit lined with a Whatman 934-AH glass microfiber to afford a clear, colorless solution. The filtrate was reduced by 50% by rotary evaporation, followed by addition of diethyl ether to afford a colorless precipitate, 216 mg (87%) of **15a**: mp 288−290 °C dec; IR (CCl_4) 3053, 2966, 1262, 1156, 1102, 1028 cm^{-1}; ^{31}P NMR (CD_2Cl_2) δ −13, J_{Pt-P} = 3041 Hz; ^{19}F NMR (CD_2Cl_2) δ −76; ^1H NMR (CD_2Cl_2) δ 9.0 (m, H_α, 16H), 7.7 (bs, 36H), 7.4 (bs, 44H), 6.9 (m, H_β, 16H), 3.3 (bs, 16H), 2.3 (m, 8H); ^{13}C NMR (CD_2Cl_2) δ 151.8 (C_α), 146.0 (C_γ), 133.5 (C_o), 132.4 (C_p), 129.6 (C_m), 125 (C_β), 124.6 (C_{ipso}), 121.3 (q, OTf, J_{C-F} = 319 Hz), 21.5 ($P(CH_2)_2$), 18.0 (CH_2). Anal. Calcd for $C_{156}H_{136}Pt_4P_8S_8N_8O_{24}F_{24} \cdot 2CH_2Cl_2$: C, 42.96; H, 3.19; N, 2.54; S, 5.81. Found: C, 42.94; H, 3.32; N, 2.59; S, 5.83.

X-ray quality crystals were grown by slow diffusion of diethyl ether into **15a** dissolved in a 1:1 mixture of CH_2Cl_2/CH_3CN under N_2 at ambient temperature.

Preparation of [Pd(4,4′-bipyridyl)(dppp)$_2$(OTf)$_2$]$_4$ (15b). In analogy with the preparation of **15a**, 306 mg (0.37 mmol) of **5c** was reacted with 65 mg (0.40 mmol) of 4,4′-bipyridine in 60 mL of CH_2Cl_2 to give an immediate color change from a bright yellow solution to a colorless solution. The reaction mixture was allowed to stir for 3 h at 25 °C and a similar workup resulted in the formation of a colorless solid, 348 mg (96%) of **15b**: mp 208−210 °C dec; IR (CCl_4) 3096, 3059, 1249, 1156, 1099, 1028 cm^{-1}; ^{31}P NMR (CD_2Cl_2) δ 9.4; ^{19}F NMR (CD_2Cl_2) δ −78; ^1H NMR (CD_2Cl_2) δ 9.0 (m, H_α, 16H), 7.6 (bs, 36H), 7.3 (m, 44H), 6.9 (m, H_β, 16H), 3.2 (m, 16H), 2.3 (m, 8H); ^{13}C NMR (CD_2Cl_2) δ 151.6 (C_α), 145.8 (C_γ), 133.4 (C_o), 132.3 (C_p), 129.7 (C_m), 125.3 (C_{ipso}), 124.0 (C_β), 121.3 (q, OTf, J_{C-F} = 319 Hz), 21.6 ($P(CH_2)_2$), 18.0 (CH_2). Anal. Calcd for $C_{156}H_{136}Pd_4P_8S_8N_8O_{24}F_{24} \cdot 2CH_2Cl_2$: C, 46.71; H, 3.47; N, 2.76; S, 6.31. Found: C, 46.56; H, 3.54; N, 2.80; S, 6.48.

Preparation of [Pt(4,4′-bipyridyl)(PEt$_3$)$_2$(OTf)$_2$]$_4$ (16a). To a 50 mL Schlenk flask, equipped with a stir bar, containing 62 mg (0.085 mmol) of **5b** in 30 mL of CH_2Cl_2 was added 15 mg (0.094 mmol) of 4,4′-bipyridine to give an immediate precipitation of a white solid. Both **5b** and **14** are very soluble in CH_2Cl_2 and $CHCl_3$ separately, but when combined the product is completely insoluble. When CH_3NO_2 was used, a secondary minor product developed. The resulting heterogeneous reaction mixture was allowed to stir at 25 °C for 1 h. The reaction mixture was then collected and washed with diethyl ether to afford a colorless precipitate, 68 mg (90%) of **16a**: mp 317−320 °C dec; IR (CCl_4) 3107, 2976, 2942, 1259, 1222, 1151, 1029 cm^{-1}; ^{31}P NMR (CD_3NO_2) δ 4.1, J_{Pt-P} = 3086 Hz; ^{19}F NMR (CD_3NO_2), δ −76; ^1H NMR δ 9.0 (d, H_α, 16H), 8.0 (d, H_β, 16H), 2.0 (t, 48H), 1.3 (m, 72H); ^{13}C NMR δ 152.4 (C_α), 146.6 (C_γ), 126.6 (C_β), 121.5 (q, OTf, J_{C-F} = 319 Hz), 17 (CH_2), 8.3 (CH_3). Anal. Calcd for $C_{96}H_{152}Pt_4P_8S_8N_8O_{24}F_{24} \cdot 4H_2O$: C, 31.90; H, 4.46; N, 3.10; S, 7.10. Found: C, 31.67; H, 4.54; N, 3.08; S, 6.88.

Preparation of [Pd(4,4′-bipyridyl)(PEt$_3$)$_2$(OTf)$_2$]$_4$ (16b). To a 50 mL Schlenk flask, equipped with a stir bar, containing 107 mg (0.17 mmol) of **5d** in 25 mL of CH_3NO_2 was added 32 mg (0.20 mmol) of 4,4′-bipyridine to give an immediate color change from a yellow solution to a colorless solution. The resulting homogeneous reaction mixture was allowed to stir at 25 °C for 2 h. The reaction mixture was reduced in volume by 75% by rotary evaporation, followed by addition of diethyl ether to afford a colorless precipitate, 119 mg (89%) of **16b**: mp 204−208 °C dec; IR (CCl_4) 3105, 2975, 2943, 1260, 1223, 1153, 1030 cm^{-1}; ^{31}P NMR (CD_3NO_2) δ 34; ^{19}F NMR (CD_3NO_2) δ −76; ^1H NMR (CD_3NO_2) δ 8.9 (d, H_α, 16H), 7.9 (d, H_β, 16H), 2.0 (t, 48H), 1.3 (m, 72H); ^{13}C NMR (CD_3NO_2) δ 152.0 (C_α), 147.0 (C_γ), 126.0 (C_β), 122.0 (q, OTf, J_{C-F} = 319 Hz), 17.2 (CH_2), 8.6 (CH_3). Anal. Calcd for $C_{96}H_{152}Pd_4P_8S_8N_8O_{24}F_{24} \cdot 4H_2O$: C, 35.37; H, 4.95; N, 3.44; S, 7.87. Found: C, 35.06; H, 4.97; N, 3.44; S, 7.84.

Preparation of [Pt(2,7-diazapyrene)(PEt$_3$)$_2$(OTf)$_2$]$_4$ (17a). In analogy with the preparation of **16a**, 97 mg (0.13 mmol) of **5b** was reacted with 31 mg (0.15 mmol) of **9** in 30 mL of CH_3NO_2 for 8 h at 25 °C. A similar workup resulted in the formation of an analytically pure, light yellow powder, 105 mg (85%) of **17a**: mp 303−307 °C dec; IR (CCl_4) 3069, 2976, 2946, 1261, 1225, 1157, 1030 cm^{-1}; ^{31}P NMR (CD_3NO_2) δ 4.4, J_{Pt-P} = 3085 Hz; ^{19}F NMR (CD_3NO_2) δ −76; ^1H NMR (CD_3NO_2) δ 10.0 (d, H_α, 16H), 8.4 (s, H_γ, 16H), 2.0 (m, 48H), 1.4 (m, 72H); ^{13}C NMR (CD_3NO_2) δ 147.0 (C_α), 130.0 (C_{ipso}), 129.7 (C_γ), 127 (C_β), 122 (q, OTf, J_{C-F} = 319 Hz), 16 (CH_2), 8.3 (CH_3). Anal. Calcd for $C_{112}H_{152}Pt_4P_8N_8S_8O_{24}F_{24} \cdot 2H_2O$: C, 35.66; H, 4.11; N, 2.97; S, 6.80. Found: C, 35.59; H, 4.14; N, 3.00; S, 6.84.

Preparation of [Pd(2,7-diazapyrene)(PEt$_3$)$_2$(OTf)$_2$]$_4$ (17b). In analogy with the preparation of **16b**, 38 mg (0.059 mmol) of **5d** was reacted with 12 mg (0.059 mmol) of **9** in 30 mL of CH_3NO_2 for 8 h at 25 °C. A similar workup resulted in the formation of an analytically pure, light yellow powder, 45 mg (91%) of **17b**: mp 189−192 °C dec; IR (CCl_4) 3070, 2972, 2945, 1266, 1224, 1156, 1030 cm^{-1}; ^{31}P NMR (CD_3NO_2) δ 34; ^{19}F NMR (CD_3NO_2) δ −76; ^1H (CD_3NO_2) 10.0 (d, H_α, 16H), 8.3 (s, H_γ, 16H), 2.0 (m, 48H), 1.4 (m, 72H); ^{13}C NMR (CD_3NO_2) δ 147.0 (C_α), 129.7 (C_{ipso}), 129.5 (C_γ), 127 (C_β), 122 (q, OTf, J_{C-F} = 319 Hz), 17.1 (CH_2), 8.6 (CH_3). Anal. Calcd for $C_{112}H_{152}Pd_4P_8N_8S_8O_{24}F_{24} \cdot 2H_2O$: C, 39.38; H, 4.60; N, 3.28; S, 7.51. Found: C, 39.25; H, 4.71; N, 3.34; S, 7.50.

Preparation of [Pt(2,9-diazadibenzo[*cd,lm*]perylene)(PEt$_3$)$_2$(OTf)$_2$]$_4$ (18a). To a 25 mL Schlenk flask, equipped with a stir bar, containing 41 mg (0.055 mmol) of **5b** in 20 mL of CH_3NO_2 was added 18 mg (0.055 mmol) of 2,9-diazaperylene, to give a heterogeneous orange solution. Within a few minutes, the 2,9-diazaperylene slowly dissolves, resulting in a homogeneous yellow/orange-colored solution, which was allowed to stir at 25 °C for 3 h. The reaction mixture was reduced in volume by 80% by rotary evaporation, followed by addition of diethyl ether to afford an orange/brown solid, 46 mg (79%) of **18a**: mp 290−296 °C dec; IR 3077, 2974, 2930, 1257, 1223, 1154, 1029 (CCl_4) cm^{-1}; ^{31}P NMR (CD_3NO_2) δ 4 (J_{Pt-P} = 3085 Hz); ^{19}F NMR (CD_3NO_2) δ −76; ^1H NMR (CD_3NO_2) δ 10.1 (d, H_α, 16H), 9.3 (d, H_β, 16H), 8.6 (d, H_γ, 16H), 2.1 (m, 48H), 1.4 (m, 72H).

Preparation of [Pd(2,9-diazadibenzo[*cd,lm*]perylene)(PEt$_3$)$_2$(OTf)$_2$]$_4$ (18b). In analogy with the preparation of **18a**, 30 mg (0.047 mmol) of **5d** was reacted with 15 mg (0.047 mmol) of 2,9-diazaperylene in 20 mL of CH_3NO_2 for 3 h at 25 °C. A similar workup resulted in the formation of an orange/brown solid, 18 mg (41%) of **18b**: IR (CCl_4) 3088, 2975, 2938, 1257, 1223, 1153, 1029 cm^{-1}; ^{31}P NMR (CD_3NO_2) δ 33; ^{19}F NMR (CD_3NO_2) δ −76; ^1H NMR (CD_3NO_2) δ 10.3 (d, H_α, 16H), 9.2 (d, H_β, 16H), 8.2 (d, H_γ, 16H), 2.0 (m, 48H), 1.3 (m, 72H).

Preparation of [(Pt(pyrazine)$_2$(dppp)(OTf)$_2$] (20a). To a solution in a Schlenk flask containing 126 mg (0.139 mmol) of **5a** in 30 mL of CH_2Cl_2 was added 33 mg (0.417 mmol) of pyrazine, to give a clear, homogeneous solution. The reaction mixture was stirred at 25 °C for 8 h. The colorless solution was filtered through a coarse-porosity glass frit lined with a Whatman 934-AH glass microfiber to afford a clear, colorless filtrate, which was concentrated to 10 mL by rotary evaporation, followed by addition of pentane to precipitate an off-white solid. Collection, washing with pentane, and drying under vacuum in a drying tube gave an off-white solid, 133 mg (90%) of **20a**: mp 253−254 °C dec; IR (CCl_4) 3045, 2965, 1260, 1155, 1102, 1030 cm^{-1}; ^{31}P NMR (CD_2Cl_2) δ −13.9 (J_{Pt-P} = 3087 Hz); ^{19}F NMR (CD_2Cl_2) δ −76; ^1H NMR (CD_2Cl_2) δ 9.0 (d, H_α, 4H), 8.4 (d, H_β, 4H), 7.7 (bm, 8H), 7.4 (bm, 12H), 3.3 (bs, 4H), 2.3 (bs, 2H); ^{13}C NMR (CD_2Cl_2) δ 149.0 (C_α), 145.2 (C_β), 133.3 (C_o), 133.1 (C_p), 129.9 (C_m), 123.8 (C_{ipso}), 121.4

(q, OTf, J_{C-F} = 318 Hz), 21.3 ($P(CH_2)_2$), 18.0 (CH_2). Anal. Calcd for $C_{37}H_{34}PtP_2S_2N_4O_6F_6 \cdot CH_2Cl_2$: C, 39.66; H, 3.15; N, 4.87; S, 5.57. Found: C, 40.13; H, 3.01; N, 3.49; S, 5.20.

X-ray quality crystals were grown by layering of pentane onto **20a** dissolved in CH_2Cl_2 at low temperature. The crystals were observed to slowly lose solvent as they became more opaque upon removal from the solvent system.

Preparation of [(Pd(pyrazine)$_2$(dppp)(OTf)$_2$] (20b). In analogy with the preparation of **20a**, 535 mg (0.655 mmol) of **5c** was reacted with 157 mg (1.96 mmol) of pyrazine in 60 mL of CH_2Cl_2, resulting in an immediate color change from yellow to a colorless solution. The reaction was allowed to stir for 8 h at 25 °C. A similar workup resulted in the formation of an off-white solid, 621 mg (72%) of **20b**: mp 246–247 °C dec; IR (CCl_4) 3040, 2969, 1265, 1153, 1105, 1030 cm^{-1}; ^{31}P NMR (CD_2Cl_2) δ 9.0; ^{19}F NMR (CD_2Cl_2) δ −76; ^{1}H NMR (CD_2Cl_2) δ 9.0 (bd, H_α, 4H), 8.3 (bd, H_β, 4H), 7.6 (bm, 8H), 7.4 (bm, 12H), 3.2 (bs, 4H), 2.3 (bs, 2H); ^{13}C NMR (CD_2Cl_2) δ 148.0 (C_α), 145.1 (C_β), 133.2 (C_o), 133.0 (C_p), 130.0 (C_m), 124.4 (C_{ipso}), 121.3 (q, OTf, J_{C-F} = 319 Hz), 21.4 ($P(CH_2)_2$), 17.9 (CH_2). Anal. Calcd for $C_{37}H_{34}PdP_2S_2N_4O_6F_6 \cdot CH_2Cl_2$: C, 42.97; H, 3.42; N, 5.28; S, 6.04. Found: C, 42.96; H, 3.33; N, 5.17; S, 6.18.

X-ray quality crystals were grown by layering of pentane onto **20b** dissolved in CH_2Cl_2 at ambient temperature.

Preparation of [Pd(1,4-dicyanobenzene)(dppp)(OTf)$_2$]$_4$ (22). In analogy with the preparation of **15a**, 141 mg (0.17 mmol) of **5c** in 20 mL of CH_2Cl_2 was reacted with 133 mg (1.04 mmol) of 1,4-dicyanobenzene in 20 mL of CH_2Cl_2 for 8 h at 25 °C. The bright yellow reaction mixture was filtered, and the filtrate was reduced in volume by 75% by rotary evaporation, followed by addition of diethyl ether to afford a yellow powder. The precipitate was collected on a medium-porosity glass frit and washed with a copious amount of diethyl ether. Crystallization from CH_2Cl_2/diethyl ether mixture afforded **22** as analytically pure, light yellow microcrystals, 158 mg (97%) of **22**: mp 275–280 °C dec; IR (CCl_4) 3095, 3056, 2280, 1257, 1222, 1148, 1027 cm^{-1}; ^{31}P NMR (CD_2Cl_2) δ 17.4; ^{19}F NMR (CD_2Cl_2) δ −76; 11H NMR (CD_2Cl_2) δ 7.7 (m, 32H), 7.6 (s, 16H), 7.5 (m, 16H), 7.4 (m, 32H), 2.9 (bs, 16H), 2.3 (m, 8H); ^{13}C NMR (CD_2Cl_2) δ 133.6 (C_α), 133.5 (C_o), 133.3 (C_p), 129.9 (C_m), 124.3 (C_{ipso}), 121.3 (q, OTf, J_{C-F} = 319 Hz), 118.4 (CN), 115.8 (C_{ipso}), 22.3 ($P(CH_2)_2$), 18.7 (CH_2). Anal. Calcd for $C_{148}H_{120}Pd_4P_8S_8N_8O_{24}F_{24}$: C, 47.02; H, 3.20; N, 2.96; S, 6.78. Found: C, 46.91; H, 3.26; N, 2.90; S, 6.70.

Preparation of [Pd(4,4′-dicyanobiphenyl)(dppp)(OTf)$_2$]$_4$ (24). In analogy with the preparation of **22**, 133 mg (0.16 mmol) of **5c** was reacted with 33.2 mg (0.16 mmol) of 4,4′-dicyanobiphenyl in 40 mL of CH_2Cl_2 for 8 h at 25 °C. A similar workup resulted in the formation of an analytically pure, yellow powder, 103 mg (62%) of **24**: mp 270–280 °C dec; IR (CCl_4) 3057, 2924, 2270, 1261, 1157, 1030 cm^{-1}; ^{31}P NMR (CD_2Cl_2) δ 16.8; ^{19}F NMR (CD_2Cl_2) δ −77; ^{1}H NMR (CD_2Cl_2) δ 7.8–7.7 (m, 32H), 7.6–7.5 (m, 16H), 7.6 (d, 16H), 7.5 (d, 16H), 7.5–7.4 (m, 32H), 2.9 (bs, 16H), 2.3 (bs, 8H); ^{13}C NMR (CD_2Cl_2) δ 144.9 (C_γ), 134.1 (C_α), 133.6 (C_o), 133.3 (C_p), 129.9 (C_m), 128.3 (C_β), 124.6 (C_{ipso}), 120.8 (CN), 120.7 (q, OTf, J_{C-F} = 318 Hz), 109.6 (C_{ipso}), 22.2 ($P(CH_2)_2$), 18.7 (CH_2). Anal. Calcd for $C_{172}H_{136}Pd_4P_8S_8N_8O_{24}F_{24}$: C, 50.57; H, 3.36; N, 2.74; S, 6.28. Found: C, 50.66; H, 3.34; N, 2.83; S, 6.39.

Preparation of [Pd$_2$(1,4-dicyanobenzene)(dppp)$_2$ (OTf)$_4$] (25). To a 50 mL Schlenk flask, equipped with a stir bar, containing 104 mg (0.13 mmol) of **5c** in 10 mL of CH_2Cl_2 was added 8 mg (0.062 mmol) of 1,4-dicyanobenzene dissolved in 20 mL of CH_2Cl_2. The resulting homogeneous yellow reaction mixture was allowed to stir at 25 °C for 8 h. The reaction mixture was filtered, and the filtrate was reduced in volume by 75% by rotary evaporation, followed by addition of diethyl ether to afford a yellow powder. Crystallization from CH_2Cl_2/diethyl ether mixture at ambient temperature afforded **25** as analytically pure, bright yellow crystals, 105 mg (94%) of **25**: mp 220–228 °C dec; IR (CCl_4) 3098, 3089, 2261, 1259, 1204, 1142, 1095, 1033 cm^{-1}; ^{31}P NMR (CD_2Cl_2) δ 18.9; ^{19}F NMR (CD_2Cl_2) δ −77; ^{1}H NMR (CD_2Cl_2) δ 7.7–7.6 (m, 16H), 7.6 (s, 4H), 7.6–7.5 (m, 8H), 7.5–7.4 (m, 16H), 2.8 (m, 8H), 2.3 (m, 4H); ^{13}C NMR (CD_2Cl_2) δ 133.7 (C_α), 133.6 (C_o), 133.3 (C_p), 129.8 (C_m), 124.1 (C_{ipso}), 120.3 (q, OTf, J_{C-F} = 318 Hz), 118.6 (CN), 115.7 (C_{ipso}), 22.5 ($P(CH_2)_2$), 18.7 (CH_2). Anal. Calcd for $C_{66}H_{56}Pd_2P_4S_4N_2O_{12}F_{12}$: C, 44.99; H, 3.20; N, 1.59; S, 7.28. Found: C, 44.75; H, 3.29; N, 1.35; S, 7.54.

X-ray quality crystals were grown by slow diffusion of diethyl ether into **25** dissolved in CH_2Cl_2 under N_2 at ambient temperature.

Preparation of [Pd$_2$(4,4′-dicyanobiphenyl)(dppp)$_2$(OTf)$_4$] (26). In analogy with the preparation of **25**, 82 mg (0.10 mmol) of **5c** in 10 mL of CH_2Cl_2 was reacted with 10 mg (0.050 mmol) of 4,4′-dicyanobiphenyl in 5 mL of CH_2Cl_2 for 8 h at 25 °C. A similar workup resulted in the formation of an analytically pure, yellow microcrystals, 63 mg (68%) of **26**: mp 271–274 °C dec; IR (CCl_4) 3070, 2265, 1436, 1313, 1258, 1209, 1189, 1031 cm^{-1}; ^{31}P NMR (CD_2Cl_2) δ 18.6; ^{19}F NMR (CD_2Cl_2) δ −76; ^{1}H NMR (CD_2Cl_2) δ 7.8–7.7 (m, 16H), 7.6–7.5 (m, 8H), 7.6 (d, 4H), 7.5–7.4 16H), 7.5 (d, 4H), 2.9 (bs, 8H), 2.3 (bs, 4H); ^{13}C NMR (CD_2Cl_2) δ 145.3 (C_γ), 134.4 (C_α), 133.6 (C_o), 133.3 (C_p), 129.9 (C_m), 128.4 (C_β), 124.5 (C_{ipso}), 121.5 (CN), 120.4 (q, OTf, J_{C-F} = 318 Hz), 108.8 (C_{ipso}), 22.4 ($P(CH_2)_2$), 18.7 (CH_2). Anal. Calcd for $C_{72}H_{60}Pd_2P_4S_4N_2O_{12}F_{12} \cdot H_2O$: C, 46.59; H, 3.37; N, 1.51; S, 6.91. Found: C, 46.83; H, 3.39; N, 1.60; S, 6.99.

Attempts at the Preparation of [Pd$_4$(1,4-dicyanobenzene)$_2$(4,4′-dicyanobiphenyl)$_2$(dppp)$_4$(OTf)$_8$]. To a 25 mL Schlenk flask containing 18 mg (0.010 mmol) of [Pd$_2$(1,4-dicyanobenzene)(dppp)$_2$(OTf)$_4$] (**25**) in 20 mL of CH_2Cl_2 was added 2.0 mg (0.010 mmol) of 4,4′-dicyanobiphenyl (**23**). The homogeneous reaction was allowed to stir for 3 h at ambient temperature. The solvent was then reduced by 50% by rotary evaporation, followed by addition of pentane to afford a light yellow-colored solid. The precipitate was collected on a medium-porosity glass frit and washed with a copious amount of pentane, followed by diethyl ether, to afford a light yellow solid, 18 mg. ^{1}H NMR, ^{31}P NMR, and IR spectra were obtained indicating that both tetrametallic molecular boxes **22** and **24** were separately formed, and none of the rectangular structure was observed. All attempts at separating the two individual components by recrystallization were unsuccessful.

Analogous to the above procedure, 33.3 mg (0.018 mmol) of [Pd$_2$(4,4′-dicyanobiphenyl)(dppp)$_2$(OTf)$_4$] (**26**) was reacted with 2.3 mg (0.018 mmol) of 1,4-dicyanobenzene (**21**) in CH_2Cl_2 at room temperature. After a similar workup, ^{1}H and ^{31}P NMR spectra along with IR spectra were taken of the isolated product (19.8 mg) which indicated a mixture of **22** and **24**. Both attempts using the dimetallic complexes **25** and **26** at preparing rectangular molecular squares with the respective 1,4-dicyanobenzene and 4,4′-dicyanobiphenyl ligands were unsuccessful as indicated by ^{1}H NMR, ^{31}P NMR, and IR spectroscopy.

Exchange Experiments of [Pd(1,4-dicyanobenzene)(dppp)(OTf)$_2$]$_4$ (22) with 4,4′-Bipyridine (14) (NMR Monitored Experiment). A 5 mm NMR tube was charged with 20 mg (0.0053 mmol) of **22**, along with 0.7 mL of CD_2Cl_2. The NMR tube was capped with a rubber septum and shaken vigorously to effect dissolution. To the bright yellow, homogeneous reaction mixture in the NMR tube was added 3.4 mg (0.022 mmol), an excess of 4,4′-bipyridine (**14**). Immediately upon addition of **14**, the reaction changes from yellow to a colorless solution, analogous to the observation for the formation of **15a**. The mixture was kept at room temperature, and the reaction was monitored by ^{1}H and ^{31}P NMR spectroscopy. Both ^{1}H and ^{31}P NMR spectra indicated a complete exchange of the 1,4-dicyanobenzene for the 4,4′-bipyridine, resulting in the formation of [Pd(4,4′-bipyridyl)(dppp)$_2$-(OTf)$_2$]$_4$ (**15b**) exclusively, and none of the tetrametallic [Pd(1,4-dicyanobenzene)(dppp)(OTf)$_2$]$_4$ (**22**) was observed to remain intact.

Likewise, a 5 mm NMR tube was charged with 26 mg (0.0069 mmol) of **22**, along with 0.7 mL of CD_2Cl_2, capped with a rubber septum, and shaken vigorously to effect dissolution. To the bright yellow, homogeneous solution in the NMR tube was added slightly less than 1 equiv (1.0 mg, 0.0068 mmol) of **14**. Immediately upon addition of **14**, the reaction changes from a yellow to a colorless solution, analogous to the above NMR tube reaction. The mixture was kept at room temperature, and the reaction was monitored by ^{1}H and ^{31}P NMR spectroscopy. ^{1}H and ^{31}P NMR spectra were consistent with [Pd(4,4′-bipyridyl)(dppp)$_2$(OTf)$_2$]$_4$ (**15b**), along with a very minor residual amount of [Pd(1,4-dicyanobenzene)(dppp)(OTf)$_2$]$_4$ (**22**).

Host–Guest Experiments Conducted with 15a,b and 17a with 1,5-Dihydroxynaphthalene. A typical experiment involved the use of a standard solution of the guest 1,5-dihydroxynaphthalene dissolved in CD_3OD. A known volume, typically 0.1 mL, was added to a 5 mm NMR tube and diluted to 0.7 mL, followed by subsequent addition of the host at various ratios, 0:1.0, 0.5:1.0, 1.0:1.0, 1.5:1.0, 2.0:1.0, 2.5:1.0, 3.0:1.0, and 3.5:1.0. The chemical shifts of the ortho and meta

Table 5. ^{1}H NMR Chemical Shift Changes (in ppm) of the Ortho and Meta Protons of the 1,5-Dihydroxynaphthalene System (**27**) with **15a**, **15b**, and **17a** at Various Host–Guest Ratios

ratio		**15a**		**15b**		**17a**	
host	guest	ortho	meta	ortho	meta	ortho	meta
0.0	1.0	0.000	0.000	0.000	0.000	0.000	0.000
0.5	1.0	0.022	0.033	0.017	0.025	0.008	0.014
1.0	1.0	0.043	0.065	0.031	0.050	0.027	0.033
1.5	1.0	0.066	0.099	0.044	0.070	0.037	0.047
2.0	1.0	0.079	0.119	0.055	0.089	0.049	0.059
2.5	1.0	0.098	0.146	0.064	0.102	0.059	0.069
3.0	1.0	0.117	0.175				
3.6	1.0	0.127	0.194				

protons of the 1,5-dihydroxynaphthalene system were observed by ^{1}H NMR spectroscopy and are summarized in Table 5.

15a. To a 5 mL volumetric flask was added 22.6 mg (0.028 25 M) of 1,5-dihydroxynaphthalene, along with CD_3OD to the appropriate level. Via syringe, 0.1 mL was removed from the flask and added to the NMR tube. A ^{1}H NMR spectrum was then obtained for this host to guest ratio of 0.0:1.0. To this solution was added 6.0 mg (0.0014 mmol) of **15a**. The NMR tube was shaken vigorously to effect dissolution, and a ^{1}H NMR spectrum was obtained for this host to guest ratio of 0.5:1.0. Subsequent ratios were obtained by addition of 6.0 mg of **15a** to the NMR tube solution.

15b. Analogous to **15a**, 20.5 mg (0.0256 M) of 1,5-dihydroxynaphthalene was dissolved in 5 mL of CD_3OD in a 5 mL volumetric flask. Via syringe, 0.1 mL of this standard solution was added to an NMR tube, followed by 5.0 mg (0.000 13 mmol) of **15b** for the varying ratios. ^{1}H NMR spectra were observed for the ortho and meta protons of the 1,5-dihydroxynaphthalene. The NMR tube solution was saturated at the 2.5:1.0 ratio.

17a. Analogous to the above experiments, 10.7 mg (0.0134 M) of 1,5-dihydroxynaphthalene was dissolved with CD_3OD in a 5 mL volumetric flask. For each subsequent host to guest ratio, 2.5 mg (0.000 67 mmol) of **17a** was added.

Acknowledgment. Financial support by the NSF (CHE-9101767) is gratefully acknowledged. S.S. thanks the Nagai Foundation of Tokyo, Japan, for financial support.

Supplementary Material Available: Positional parameters and ESD, anisotropic displacement parameters, and an extended list of bond lengths, bond angles, and torsion angles for compounds **15a**, **20a,b**, and **25** (48 pages). This material is contained in many libraries on microfiche, immediately follows this article in the microfilm version of the journal, can be ordered from the ACS, and can be downloaded from the Internet; see any current masthead page for ordering information and Internet access instructions.

JA950788Z